

# High throughput drug discovery with ESI-FTICR

Kristin A. Sannes-Lowery\*, Lendell L. Cummins,  
Shuo Chen, Jared J. Drader, Steven A. Hofstadler

*Ibis Therapeutics, Division of Isis Pharmaceuticals, 2292 Faraday Avenue, Carlsbad, CA 92008, USA*

Received 1 February 2004; accepted 1 April 2004

Available online 28 September 2004

## Abstract

Ribonucleic acids (RNA) are an attractive target for drug discovery since they play critical roles in cellular functions. Because small structured subdomains are known to mimic the behavior of the entire RNA, it is possible to design RNA drug targets that are amenable to interrogation by high performance mass spectrometry. We have developed a high throughput drug discovery platform that uses electrospray ionization Fourier transform ion cyclotron mass spectrometry to investigate ligand binding to structured RNA drug targets. This assay is called multitarget affinity/specificity screening (MASS). Using MASS, we show that it is possible to screen synthetic and natural product libraries in a high throughput and robust manner.

© 2004 Elsevier B.V. All rights reserved.

*Keywords:* Drug discovery; ESI FTICR mass spectrometry; RNA; Noncovalent complexes

## 1. Introduction

Ribonucleic acids (RNA) are an attractive target for therapeutic intervention in a variety of diseases such as bacterial infections, viral infections, cancer, inflammation and neurological disorders. RNA performs a variety of critical functions in the cell including peptide bond formation, messenger RNA (mRNA) splicing, transfer RNA (tRNA) transport and regulation of both transcription and translation. Although RNA has only four building blocks, a plethora of structural diversity, arguably equivalent to that of protein targets, is generated. The three-dimensional structure of RNA is required for both molecular recognition and functionality [1]. To maintain the functional structures, little or no change can be tolerated at active sites in ribosomal RNA (rRNA) and at protein-binding regions of mRNA molecules. Therefore, it is difficult for pathogens to develop resistance to drugs targeted at structured RNAs [2]. Recent advances in the determination

of RNA structure and function make targeting unique RNA motifs with small molecules a tractable problem [3–5].

Nature has provided examples of small molecules that exhibit a therapeutic effect by binding to structured RNAs. One of the most studied ligand–RNA systems is the binding of aminoglycoside antibiotics to the Prokaryotic 16S rRNA. The 16S rRNA sequence is highly conserved among prokaryotes and is part of the 30S subunit involved in translation. The therapeutic effect of aminoglycoside antibiotics is due to disruption of protein synthesis and RNA splicing. One of the best characterized aminoglycoside binding sites is the A-site domain of the 16S rRNA [6–17]. This binding site has been studied by NMR, crystallographic, and mass spectrometric techniques. A 27-mer RNA construct that comprises the A-site subdomain has been shown to mimic the behavior of the A-site domain in the entire 16S rRNA (~1500 nucleotides) [18]. The aminoglycoside paromomycin binds both the 27-mer construct and the 16S rRNA with similar affinities [11]. Additionally, NMR structures of paromomycin with the 27-mer construct have been solved and are similar to the crystal structures of the 30S subunit with paromomycin [6,13]. Since small subdomains can mimic the functional domain of rRNA,

\* Corresponding author. Tel.: +1 760 603 2453.

E-mail address: [klowery@isisph.com](mailto:klowery@isisph.com) (K.A. Sannes-Lowery).

it is possible to design RNA constructs that are amenable to analysis by high performance mass spectrometry [18].

We have developed a mass spectrometry based approach for discovery of small molecule drugs that work by binding to structured regions of RNA. This approach is called multitarget affinity/specificity screening (MASS) and employs electrospray ionization Fourier transform ion cyclotron resonance mass spectrometry (ESI-FTICR-MS) [19–21]. In a single assay, MASS can be used to determine the chemical composition of ligands that bind to an RNA target, relative/absolute dissociation constants, and the specificity of binding to one RNA target relative to other RNA targets. Because the ESI-FTICR-MS experiment provides a “snap-shot” of the species present in the solution, solution dissociation constants can be measured from the observed ion abundances of the free and complexed RNA [22]. Ligand–RNA complexes with affinity ranging from 10 nM to at least 1 mM can be observed in the MASS assay [19–21,23].

In this paper, we will describe two operating modes of MASS. First, MASS is used as a high throughput affinity screen in which compounds libraries (or natural product extracts) are assayed for compounds that bind the RNA target. Once lead compounds are identified, then MASS can be run in a mode that rapidly determines dissociation constants for target–ligand interactions to guide medicinal structure–activity relationship (SAR) efforts to optimize lead ligands. We will also show examples from screening a natural products broth and natural products extracts.

## 2. Experimental

### 2.1. Instrumentation

The mass spectrometer used in this work is based on a Bruker Daltonics (Billerica, MA) Apex II 70e electrospray ionization Fourier transform mass spectrometer that employs an actively shielded 9.4 T superconducting magnet. The active shielding constrains the majority of the fringing magnetic field from the superconducting magnet to a relatively small volume. Thus, components, which might be adversely affected by stray magnetic fields, such as CRT monitors, robotic components, and other electronics, can operate in close proximity to the spectrometer. All aspects of pulse sequence control and data acquisition are performed on a 600 MHz Pentium II datastation running Bruker Xmass software under Windows NT 4.0 operating system. Sample aliquots, typically 12  $\mu$ L, are extracted directly from 96-well microtiter plates using a CTC HTS PAL autosampler (LEAP Technologies, Carrboro, NC) which is triggered by the datastation. Samples are injected directly into a sample loop integrated with a fluidics handling system. Ions are formed via electrospray ionization in a modified Analytica (Branford, CT) source employing an off axis, grounded electrospray probe positioned ca. 1.5 cm from the metalized terminus of a glass desolvation capillary. The atmospheric pressure end of the

glass capillary is biased at 6000 V, relative to the ESI needle during data acquisition. A room-temperature counter-current flow of a 50/50 mixture of N<sub>2</sub> and O<sub>2</sub> is employed to assist in the desolvation process and to stabilize the electrospray plume. Ions are accumulated in an external ion reservoir comprised of an rf-only hexapole, a skimmer cone, and an auxiliary gate electrode, prior to injection into the trapped ion cell where they are mass analyzed. Typically, one well is screened every 39 s ( $\sim$ 1 plate/h); 33 s of data acquisition (20 coadded scans) and 6 s of overhead associated with the autosampler.

With the mass spectrometer operating in the positive ion mode, accurate mass measurements of natural product fractions were performed using angiotensin and bradykinin peptides as internal mass standards. The mass accuracy attained using these standards was  $\leq$ 1 ppm. Samples were infused at 100  $\mu$ L/h in 1% formic acid/25% isopropanol.

MS and MS<sup>n</sup> experiments were performed on a Bruker Esquire 3000 quadrupole ion trap mass spectrometer (Bruker Daltonics, Billerica, MA, USA). Fractions were infused in 1% formic acid/25% isopropanol at a rate of 2  $\mu$ L/min. MS<sup>n</sup> experiments were performed using a fragmentation amplitude that ranged from 0.7 to 1.0.

### 2.2. Materials

A 27-mer nucleotide RNA (MW<sub>min</sub> = 8635.1790 Da) that contained the essential components of the 16S rRNA A-site, **16S**, and a 28-mer nucleotide control RNA (MW<sub>min</sub> = 9300.3388 Da), **16Sc**, (Fig. 1) were obtained from Dharmacon Research, Boulder, CO. The **16Sc** construct contains an 18-atom hexaethylene glycol chain attached to the 5' terminus of the oligonucleotide as supplied by the manufacturer. The RNA was deprotected according to the manufacturer's directions and ethanol precipitated twice from 1 M ammonium acetate. Paromomycin (MW = 615.2963 Da) was obtained from Sigma (St. Louis, MO) and used without further purification.

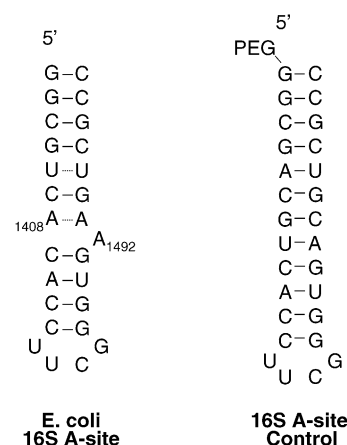


Fig. 1. Sequence and secondary structures of the 27-mer 16S A-site RNA construct (**16S**) and the 28-mer control RNA construct (**16Sc**) in which the internal bulge of **16S** has been replaced with a duplex region. Base numbering is in reference to full length *E. coli* 16S rRNA.

### 2.3. Natural products broth preparation

A dried sample of American Type Culture Collection 14827 (ATCC14827), *Streptomyces rimosus* sp. *paromomycinus*, was dissolved and resuspended in 1 mL of growth media (24 g corn meal, 11 g soybean flour, 4 g NH<sub>4</sub>Cl, 15 g CaCO<sub>3</sub>, 0.2 g MgSO<sub>4</sub>, 50 g D-glucose, 5 g soya oil in 1 L H<sub>2</sub>O). One third of the suspension was used to inoculate 25 mL of sterile media in a 200-mL baffled flask. The culture was incubated in a shaker set at 30 °C, 220 rpm for 4 days. Cells and insoluble media components were spun down and supernatant was collected. In preparation for HPLC fractionation, the supernatant was brought to 0.1% heptafluorobutyric acid (HFBA) by the addition of 1% HFBA. Three millilitres of sample were injected into a 250 mm × 10 mm Phenomenex Aqua C18 column, with a 50 mm × 10 mm guard column. Components were eluted using 0.1% HFBA and a gradient of 0–40% acetonitrile (ACN) at a flow rate of 3 mL/min over 45 min. One millilitre fractions were collected every 20 s. Two microlitre aliquots of each LC fraction was combined with a 15 µL solution containing 2.5 µM each **16S** and **16Sc** in 100 mM ammonium acetate and 33% isopropyl alcohol. This mixture was vortexed and incubated for 60 min at room temperature prior to MASS analysis.

## 3. Results and discussion

### 3.1. MASS as a high throughput screen

The MASS screen uses high performance ESI-FTICR-MS to interrogate the interaction of ligands with structured RNA targets. Because of the high mass accuracy of FTICR-MS, the exact mass of a small molecule can be used as an “intrinsic mass label” for identification of molecules that bind a target. Unlike traditional biological assays, neither the target nor the ligands require radiolabeling or fluorescent tagging to be screened. Additionally, complicated mixtures of ligands can be screened simultaneously; compounds that bind the RNA target are directly identified without deconvolution of the mixture and/or rescreening the ligands as individual compounds. Furthermore, the false positives that are observed in traditional biological assays due to an aggregate effect of a mixture is avoided in the MASS screen since each ligand has the opportunity to interact with the RNA target (see below).

Low affinity ligands (dissociation constants greater than 100 µM), which would be missed with traditional biological assays, will be identified with the MASS assay. Griffey et al. demonstrated that 2-deoxystreptomycin (2-DOS) binds to the 27-mer 16S A-site construct at multiple locations with dissociation constants ( $K_d$ ) ranging from 0.6 to 15 mM [24]. This work also demonstrates that the MASS assay can be used to examine concurrent and competitive binding of low affinity compounds [24]. An example of concurrent binding was demonstrated by the simultaneous binding of 2-DOS and 3,5-diaminotriazole (3,5-DT) to **16S** inferring that 2-DOS and

3,5-DT must bind the **16S** in different locations. Alternatively, an example of competitive binding was demonstrated by the absence of 2,4-diaminopyrimidine (DAP) binding to **16S** in the presence of 2-DOS which indicated that 2-DOS and DAP bind to **16S** in the same or overlapping locations.

To multiplex the MASS approach and make it truly high throughput, it must be possible to screen multiple targets against multiple ligands in a single well. This ability requires that the molecular interaction between any given target–ligand pair is independent of the presence (or absence) of other ligands and targets in solution. In previous work [21], we demonstrated that lividomycin will bind specifically the 27-mer 16S A-site construct in the presence of two other RNA targets and 25 compounds even when the concentration of lividomycin (3 µM) is significantly lower than the total concentration of the other ligands (1.25 mM total). Therefore, the MASS technique can characterize the interactions of complex target/ligand mixtures. Currently, three targets at 2.5 µM each are screened against 11 ligands at 25 µM each. The RNA concentration ensures that there is enough RNA available for all potential binders to interact with the RNA. The high ligand concentration ensures that even ligands with  $K_d$  values of 1 mM will be detected. Thus, in a 24-h period, 22.5 K compounds are screened and 67 K analyses are performed which requires highly automated data collection and data analysis. This approach is described in detail elsewhere [21].

In the high throughput mode, the goal is to identify ligands with  $K_d$  values less than 100 µM and with some specificity relative to the other targets. These constraints ensure that the ligands bind to a unique structural feature of the target and are not just generic RNA binders. Although the ligands are screened only at a single concentration in the high throughput mode, it is possible to estimate a one point  $K_d$  from the mass spectrometry data. A percent complex is calculated for each identified ligand–target combination by calculating the ratio of the integrated peak areas of the free and complexed target and multiplying by 100. A one point estimated  $K_d$  is then calculated by dividing 100 by the percent complex of the ligand and multiplying by the screening concentration. The one point estimated  $K_d$  values can be used to classify compounds as weak, medium, and strong binders but cannot be used to accurately rank order compounds within the same classification. As illustrated in Fig. 2a, a ligand binds target 2 with one point estimated  $K_d$  of 37 µM (i.e., estimated  $K_d = 100/67 \mu\text{M} \times 25 \mu\text{M}$ ). The ligand binds target 2 with a 3.4 greater specificity than target 1 and with 1.5 greater specificity than target 3. This ligand would be a candidate for further SAR by medicinal chemistry to improve both its binding affinity and specificity. An example of a generic RNA binder is shown in Fig. 2b. The ligand binds target 1 and target 2 equally well. In addition, complexes formed by binding two ligands to the target are observed for both target 1 and target 2. This result indicates that there are multiple weak binding sites with similar affinities for the ligand on the targets. It would likely be difficult to improve the affinity and

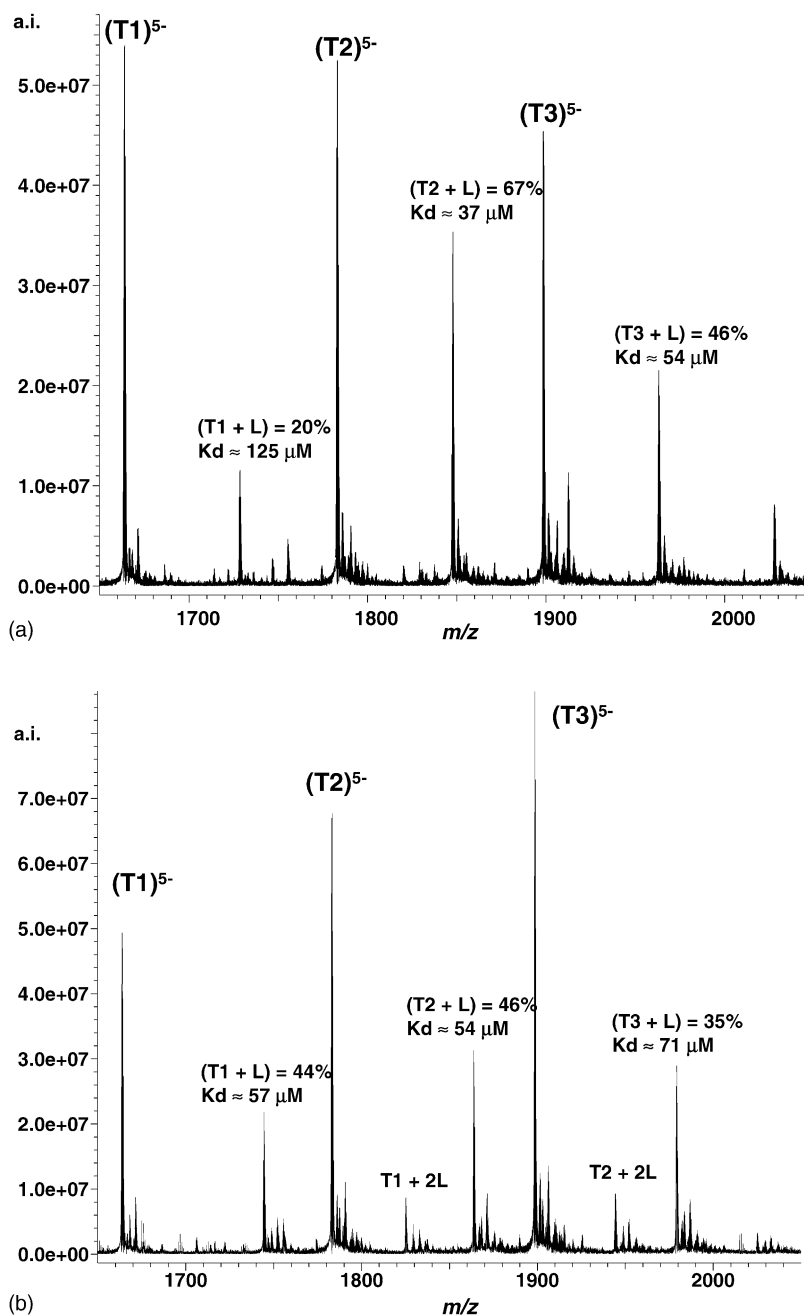


Fig. 2. ESI-FTICR mass spectra of 3 RNA targets at  $2.5 \mu\text{M}$  each screened against 11 compounds at  $25 \mu\text{M}$  each. The percent complexes and one point  $K_d$  values are shown for each ligand complex. (a) An example of a ligand that specifically binds target 2. (b) An example of a ligand that nonspecifically binds to all targets.

specificity of this ligand, and therefore, it would probably not be pursued further as a drug candidate. Thus, MASS can be used to rapidly identify promising compounds and/or structural motifs from large chemical libraries.

### 3.2. MASS for automated $K_d$ determination

It has been demonstrated that mass spectrometry can be used to characterize binding properties and stoichiometry for protein–protein interactions, protein–ligand interactions,

protein–oligonucleotide interactions, DNA–ligand interactions and RNA–ligand interactions that are in good agreement with those derived from more conventional solution phase techniques [25–39]. Several groups have shown that  $K_d$  values can be directly derived from ESI-MS measurements [25–27,32,35,36]. Traditional solution phase methods such as radioimmunoassays, filter assays, and surface plasmon resonance assays, provide little to no information about the binding stoichiometry and can only measure the equilibrium concentration of one component [40]. In contrast, mass

spectrometry can directly determine the binding stoichiometry by measuring the masses of the complexes formed as well as detect all the components of the equilibrium mixture (i.e., free ligand, free target, and ligand–target complexes). In addition, using appropriate solution conditions, it is possible to measure simultaneously the  $K_d$  values for several ligands against a single target [19] and it is possible to measure simultaneously the  $K_d$  values for a single ligand to multiple targets (unpublished results). Furthermore, it is possible to easily explore the effect of solution conditions on the measured  $K_d$  values using mass spectrometry. This is important because the  $K_d$  values for ligands with a specific binding site will not be affected by changes in salt concentration while  $K_d$  values for ligands with nonspecific binding sites can be significantly influenced by the salt concentration [22].

In previous work, we used ESI-MS to measure the  $K_d$  values for the aminoglycosides tobramycin and paromomycin binding to a 27-mer construct of the 16S A-site [22]. Equations for determining  $K_d$  values for a ligand with a single binding site (Eq. (1)) and with two binding sites (Eq. (2)) were derived since the mass spectrometry data provide information about the binding stoichiometry of the ligands.

$$\frac{[RL]}{[R]} = \left( \frac{1}{K_d} \right) ([L]_i - [RL]) \quad (1)$$

$$\frac{[RL] + [RL_2]}{[R]} = \frac{[L]^2}{K_{d1}K_{d2}} + \frac{[L]}{K_{d1}} \quad (2)$$

In eqs. (1) and (2),  $R$  is the free RNA target,  $L$  is the free ligand,  $RL$  is the 1:1 ligand–RNA target complex and  $RL_2$  is the 2:1 ligand–RNA target complex. In each equation, the mass spectrometrically determined abundances of the appropriate species are used. It was demonstrated that holding the RNA concentration fixed at or below the expected  $K_d$  value and titrating the ligand is the preferred method for determining dissociation constants. To aid our drug discovery efforts, an automated method of rapidly determining  $K_d$  values for ligands was developed.

Once promising ligands have been identified in the high throughput mode of MASS, medicinal chemistry and organic synthesis is employed for SAR studies of these compounds. These second generation collections of compounds may contain numerous active compounds with minor differences in affinity. At this point, the goal is to accurately rank order the affinities and specificities of these new compounds. Because the modifications may cause subtle differences in binding affinities, a multi-point  $K_d$  determination is necessary. An accurate  $K_d$  measurement requires that the RNA concentration used is below the expected  $K_d$ , which, for some classes of compounds is in the low nM regime. Since  $K_d$  determinations are generally done one ligand at a time, well-to-well carryover of both ligand and RNA must be minimized so that the  $K_d$  determination of one ligand does not interfere with that of another ligand.

If the estimated  $K_d$  values are in the micromolar range, the RNA is held at 500 nM concentration and the ligand is

screened at 750 nM, 2.5  $\mu$ M, 7.5  $\mu$ M and 25  $\mu$ M. Using these concentrations, it is possible to maintain the 39 s/well screening rate used in the high throughput mode. On the other hand, if the estimated  $K_d$  values are in the mid-nanomolar range, the RNA concentration is held at 100 nM and the ligand is screened at 250 nM, 750 nM, 2.5  $\mu$ M, and 7.5  $\mu$ M. At this RNA concentration, the number of scans collected to maintain the necessary signal-to-noise level is increased from 20 to 64 scans and the screening time per well goes from 39 to 95 s. For all  $K_d$  determinations, one ligand is screened per row of a 96 well microtiter plate starting with the lowest concentration. Between each ligand concentration, two wells of RNA only are run to scavenge any residual ligand in the transfer lines and to minimize ligand carryover within the row. It was found that ligand carryover within the same row interfered with the  $K_d$  determination of micromolar binders but not submicromolar binders. Furthermore, after the highest concentration is screened, two additional rinse steps are done to help minimize the carryover of the ligand to the next row, which would interfere with the next  $K_d$  determination.

The  $K_d$  values are determined by plotting the fraction of RNA bound by the ligand (fraction bound) versus the total ligand concentration. The fraction bound is determined by dividing the abundances of the ligand–RNA complexes (1:1 and 2:1 ligand–RNA complexes) by the total abundance of the RNA. The fraction bound is related to the  $K_d$  using the following equation:

$$Y = \frac{[L]_f}{K_d + [L]_f} \quad (3)$$

where  $Y$  is the fraction bound and  $[L]_f$  is the free ligand concentration. The free ligand concentration is calculated from:

$$[L]_f = [L]_i - Y[R]_i \quad (4)$$

where  $[L]_i$  is the initial ligand concentration and  $[R]_i$  is the initial RNA concentration. At a ligand concentration of zero, the fraction bound is zero by definition. Thus, zero ligand concentration can be used as an additional data point when the calculations are performed. Non-linear regression analysis is used to calculate the  $K_d$  values and curve fits with  $R^2 > 0.99$  are obtained. The above equations only calculate the  $K_d$  for the first binding site. This method for  $K_d$  determination is reproducible and robust, providing accurate  $K_d$  values for rank ordering ligands that show the subtle effects of modifications.

Using the MASS assay, the  $K_d$  values for paromomycin, kanamycin A and neamine were determined. **16S** was held at 100 nM while the aminoglycoside antibiotics were screened at 250 nM, 750 nM, 2.5  $\mu$ M and 7.5  $\mu$ M. Fig. 3 shows a plot of the fraction of **16S** bound by the ligand (fraction bound) versus the total ligand concentration for the three aminoglycosides. The  $K_d$  values determined for paromomycin (83.9 nM), kanamycin A (7.8  $\mu$ M), and neamine (13.1  $\mu$ M) are consistent with solution phase determinations [7,11] and our previous ESI-MS measurements [22]. Each  $K_d$  determination took 380 s of data acquisition, and thus, the MASS assay provides

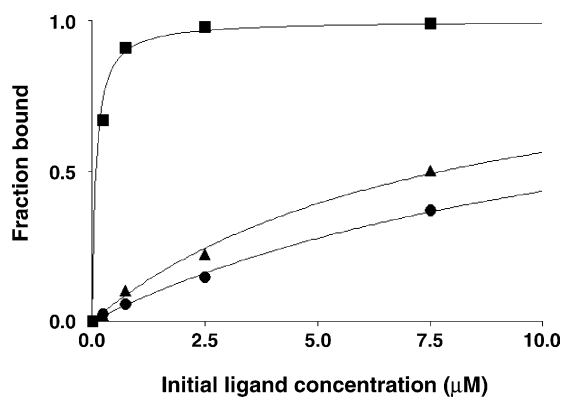


Fig. 3.  $K_d$  determination for paromomycin (■), kanamycin A (▲), and neamine (●). 16S was held at 100 nM concentration while the aminoglycosides were screened at 250 nM, 750 nM, 2.5  $\mu$ M, and 7.5  $\mu$ M. The fraction bound is plotted versus the initial ligand concentration. Nonlinear regression was used to calculate the  $K_d$  and the curves were fit with  $R^2 > 0.99$ .

a robust way to determine dissociation constants for 100 compounds a day.

### 3.3. MASS for screening natural products

Natural products provide a depth and diversity of compounds that have potential value as therapeutic drugs. In fact, for the past 20 years, natural products have been the source of many of the top selling prescription drugs. However, determining the biologically active components from natural product broths and extracts presents many challenges when using traditional biological assays. The many issues include detection of active compounds present at low concentrations in a background of other active species and “false” positives resulting from the summed activity of many weakly active compounds. The determination of the active component is often labor intensive and requires large amounts of the fractionated broth or extract. The MASS assay is ideally suited for screening very complex biologically derived mixtures, such as cell lysates, bacterial broths, and plant extracts, for individual components that bind specifically to biological targets. Because of the small amount of material required for the MASS assay, it is possible to screen the fractionated broths or extracts at multiple concentrations against multiple targets. The use of multiple concentrations ensures that even low abundance species that bind will be detected in the presence of high abundance species that bind. In addition, since the active component is identified by its molecular weight, this information greatly aids the identification process.

We recently extended the MASS assay to screening of natural product broths [41]. As a proof of principle concept, fractionated broths from *S. rimus sp. paromomycinus*, which are known to produce the aminoglycoside paromomycin, were screened against a 27-mer 16S A-site RNA construct (16S) and a 28-mer control RNA construct (16Sc) in which the 16S construct was modified to change the internal bulge into a duplex region. By screening against these two targets simul-

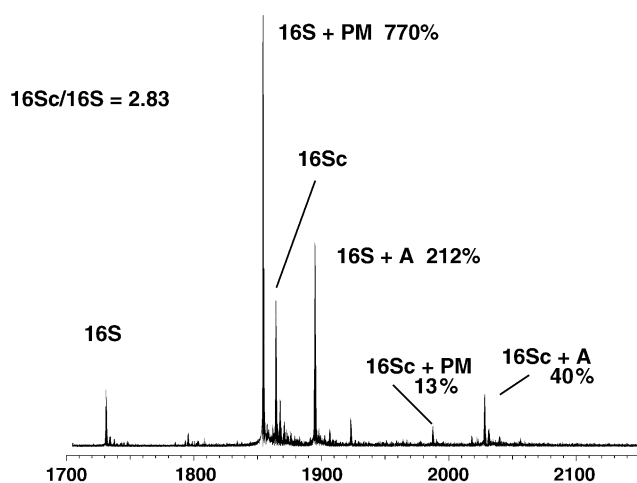


Fig. 4. ESI-FTICR mass spectrum that shows the binding species in fraction 146 (see text). Two species were observed to bind to the 27-mer 16S A-site construct (16S): (1) paromomycin (PM) and (2) Ligand A (A) that has a mass of 818 Da. The percentages shown are relative to the 16S or 16Sc targets, respectively.

taneously, ligands that bind specifically to the internal bulge of 16S can be identified. If a ligand binds equally well to both constructs, the ligand probably does not bind to internal bulge of the 16S but to a duplex region or the loop region that the two constructs have in common. The ratio of the abundance of 16Sc to 16S can be used to monitor the specificity of ligand binding. If the ligand binds the 16S specifically, the 16Sc/16S ratio will increase since the abundance of 16S will decrease relative to that of 16Sc. Conversely, if a ligand binds the two targets equally well, the 16Sc/16S ratio will not change since the abundance of both 16S and 16Sc will decrease. Similarly, in the absence of ligand binding to either target, the 16Sc/16S ratio will not change.

A bacterial fermentation broth from *S. rimus sp. paromomycinus* was fractionated using HPLC and the individual fractions were screened against the 27-mer 16S A-site RNA construct and the 28-mer 16S control RNA construct. MASS analysis of fraction 146 (~54.7 min) is shown in Fig. 4. The peak at  $m/z$  1849.90 corresponds to a ligand of mass ~615 Da binding to 16S and is putatively assigned as the 16S–paromomycin noncovalent complex. In addition, a low abundance peak corresponding to paromomycin–16Sc complex is observed at  $m/z$  1982. The peak at  $m/z$  1890.52 represents either a ligand of mass of ~818 Da complexed with 16S or a ligand of mass ~153 Da complexed with 16Sc. Further examination of the mass spectrum shows a peak at  $m/z$  2023 which corresponds to a ligand of mass ~818 Da binding to 16Sc. Because ligands that bind RNA typically will bind non-specifically to all RNAs to some extent, the above identification of  $m/z$  2023 helps identify the peak at  $m/z$  1890.52 as a ligand of mass ~818 binding to 16S. The new species with a mass of ~818 will be referred to as Ligand A in further discussions. Based on the abundances of the paromomycin–16S complex and the paromomycin–16Sc complex (Fig. 4), paromomycin binds approximately 59-fold more specifically to

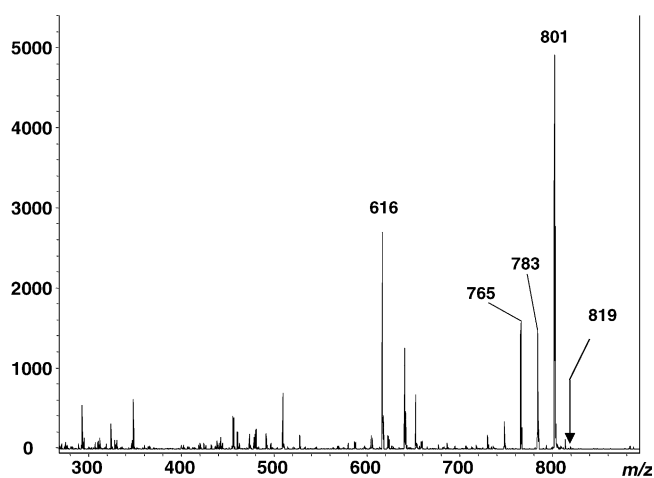


Fig. 5. MS<sup>2</sup> spectrum of **Ligand A** ( $m/z$  819) present in fraction 146. The primary fragments are loss of water to produce  $m/z$  801 and loss of 203 to produce  $m/z$  616, the paromomycin core.

the **16S** than it does to **16Sc**. A similar comparison of the **Ligand A** indicates that it binds with approximately a five-fold specificity to the **16S** over the **16Sc**.

Fraction 146 was further characterized by positive mode electrospray MS using a quadrupole ion trap mass spectrometer. The components observed in this fraction include the ( $M + H^+$ ) species of paromomycin ( $m/z$  616), the ( $M + H^+$ ) species of **Ligand A** ( $m/z$  819), and several other species that do not bind to **16S** or **16Sc** (data not shown). Paromomycin and **Ligand A** were the most abundant peaks detected and assuming comparable ionization efficiencies, are likely present at similar concentrations.

The ~615 Da species putatively identified in fraction 146 as paromomycin was confirmed by comparing its MS/MS spectra with that of commercially available paromomycin. Identical product ions were observed in the MS/MS spectra. Additionally, the fragmentation patterns observed are consistent with other studies of fragmentation pathways of paromomycin [42–44].

To obtain structural information, MS<sup>*n*</sup> was performed on **Ligand A**. The MS/MS spectrum of **Ligand A** contains a product ion at  $m/z$  616 as well as up to three losses of water ( $m/z$  801, 783, and 765) (Fig. 5). Further fragmentation of the ion at  $m/z$  616 gave product ions consistent with those found for paromomycin. This data indicates that **Ligand A** is a modified paromomycin derivative. Additional fragmentation experiments were carried out to identify the location of the modification. The MS<sup>3</sup> fragmentation of the product ion at  $m/z$  801 gave ions consistent with losses of the A ring ( $m/z$  640), the D ring ( $m/z$  641) and the CD rings ( $m/z$  509) of paromomycin (Fig. 6a). The MS<sup>4</sup> fragmentation of the product ion at  $m/z$  509 gave ions consistent with the loss of the A ring of paromomycin ( $m/z$  348). The MS<sup>5</sup> fragmentation of the product ion at  $m/z$  348 gave an ion consistent with the B ring of paromomycin ( $m/z$  163) (Fig. 6b). All of the fragmentation patterns are consistent with the modification being located on the B ring of paromomycin. All of the

MS<sup>*n*</sup> data was collected from the initial fractionation of the natural product broth and required very little material. The initial assignment of the modification being on the B ring will greatly aid further efforts to determine the exact nature of the modification.

In addition to the structural information obtained from the MS<sup>*n*</sup> data, an accurate mass measurement of **Ligand A** was performed to determine the elemental composition of the modification. The mass of this species was measured to be 819.3828 with a sub-ppm mass measurement error. The elemental composition that is consistent with the observed mass (assuming only C, H, N, and O atoms) is C<sub>31</sub> H<sub>59</sub> O<sub>19</sub> N<sub>6</sub> with a mass difference of 0.2 ppm. Since **Ligand A** is consistent with a modified paromomycin, subtracting the elemental composition of paromomycin (C<sub>23</sub> H<sub>46</sub> O<sub>14</sub> N<sub>5</sub>) from the determined elemental composition of **Ligand A**, will give the elemental composition of the modification. Thus, the elemental composition of the modification is C<sub>8</sub> H<sub>13</sub> O<sub>5</sub> N. Scale-up and isolation of **Ligand A** for NMR studies is required to determine the exact structure of the modification.

#### 3.4. MASS as a screen for enzymatic activity

In addition to finding small molecules that bind RNA, MASS can be used to find compounds that exhibit functional activity similar to that of cleavage enzymes. If the functional activity is specific for a structured RNA target, then the compound may exhibit a therapeutic effect by degrading the RNA and thus preventing the translation of a protein necessary for cell life. Unlike the previous examples of the MASS assay where small molecules are identified from the complexes that are formed with the specific RNA target, selective degradation of one RNA target relative to another is evaluated by measuring the abundance of the intact RNA target and concomitantly monitoring the ratio of the abundances of the two targets. For example, an increase in the ratio of **16Sc**/**16S** can also indicate a well where the **16S** has been preferentially degraded relative to the **16Sc**. In this case, the **16Sc** may be more difficult to degrade since it has a PEG linker on the 5' end and a fully Watson-Crick based-pair stem structure. Examples of selective degradation of **16S** were observed in fractionated broths from *S. rimus* sp. *Paromomycinus* [41]. Based on the elution profile of the fractions that showed selective degradation, it does not appear that the activity was due to proteinaceous RNases. Additional examples have been observed from fractionated plant extracts that were treated with proteases as well as from plant extracts using solvents that are not expected to solubilize proteins.

For example, Fig. 7 shows a well that exhibited selective degradation of the **16S** construct. This well contained compounds extracted from a plant using hexane in which proteins are not expected to be soluble. The natural product extract was screened at 5×, 10×, 50× dilutions from the stock concentration (25 mg/mL) and selective degradation of **16S** is observed at all concentrations. Since the

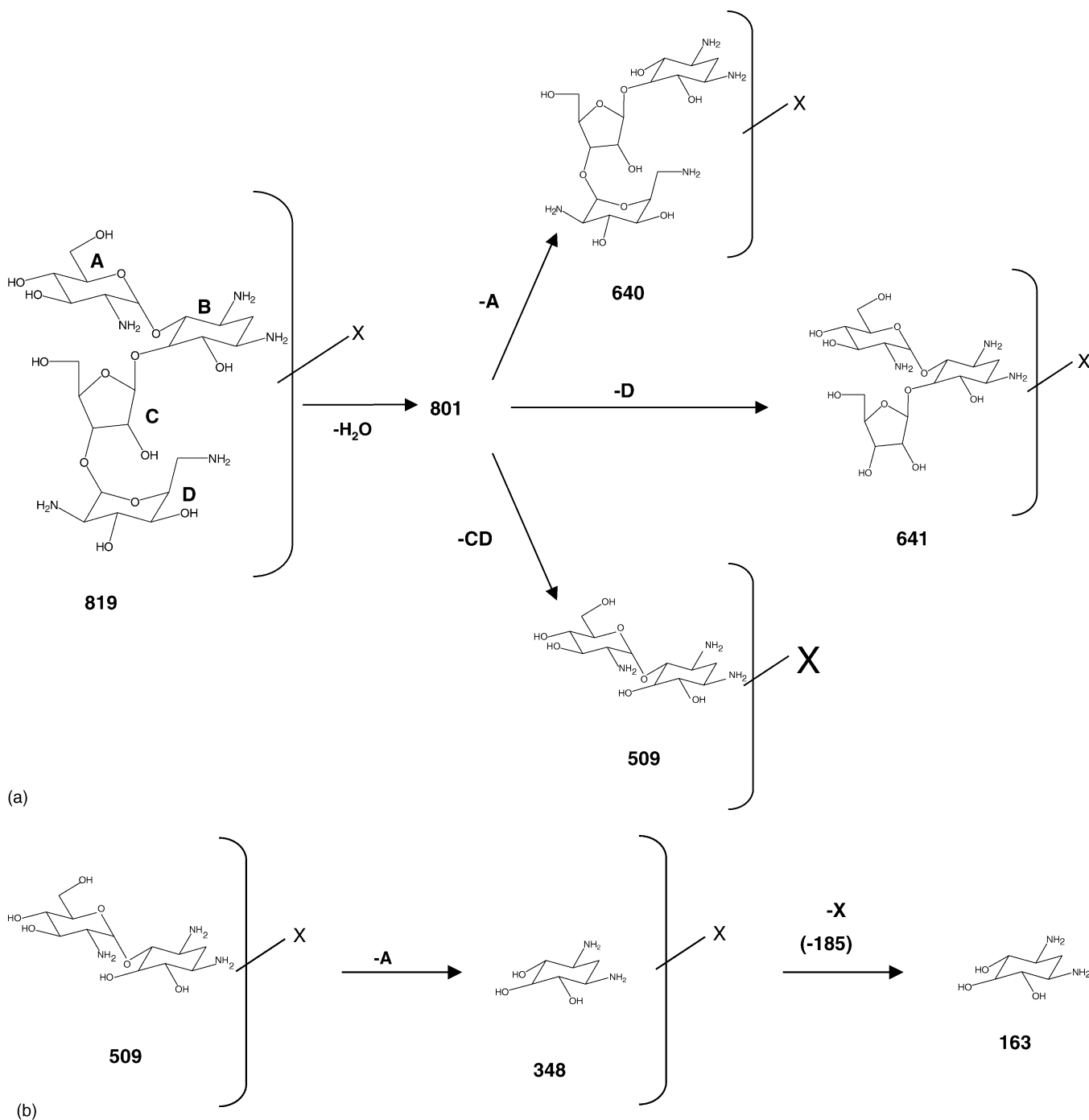


Fig. 6. Fragmentation pathways of **Ligand A**, which is a modified paromomycin. The X represents the modification to paromomycin. (a) the MS<sup>2</sup> and MS<sup>3</sup> fragmentation pathways and (b) the MS<sup>4</sup> and MS<sup>5</sup> fragmentation pathways of **Ligand A**.

abundance of **16Sc** only decreases significantly at the highest concentration screened ( $5\times$  dilution); the decrease in the abundance of **16S** is most likely due to cleavage and not overall signal degradation. The  $50\times$  dilution gives three cleavage products consistent with **16S** fragments. Based on the accurate mass of the cleavage products, base compositions were derived for the three cleavage products [45]. Using the calculated base compositions, it was determined that a cleavage occurred at the 3' side of the 1407C as indi-

cated by the product with mass 1951 which corresponds to the 5'-GGCGUC-cp and the product with mass 6683 which corresponds to -HO-ACACCUUCGGGUGAAGUCGCC-3' (Fig. 8). After this initial cleavage, it appears that the 6683 product is further cleaved at position 1496C to give HO-ACACCUUCGGGUGAAGUC-cp. It is also interesting to note that at the highest concentration of the extract, cleavage products that are consistent with cleavage of a C from **16Sc** are observed in addition to the cleavage of **16S**. Further



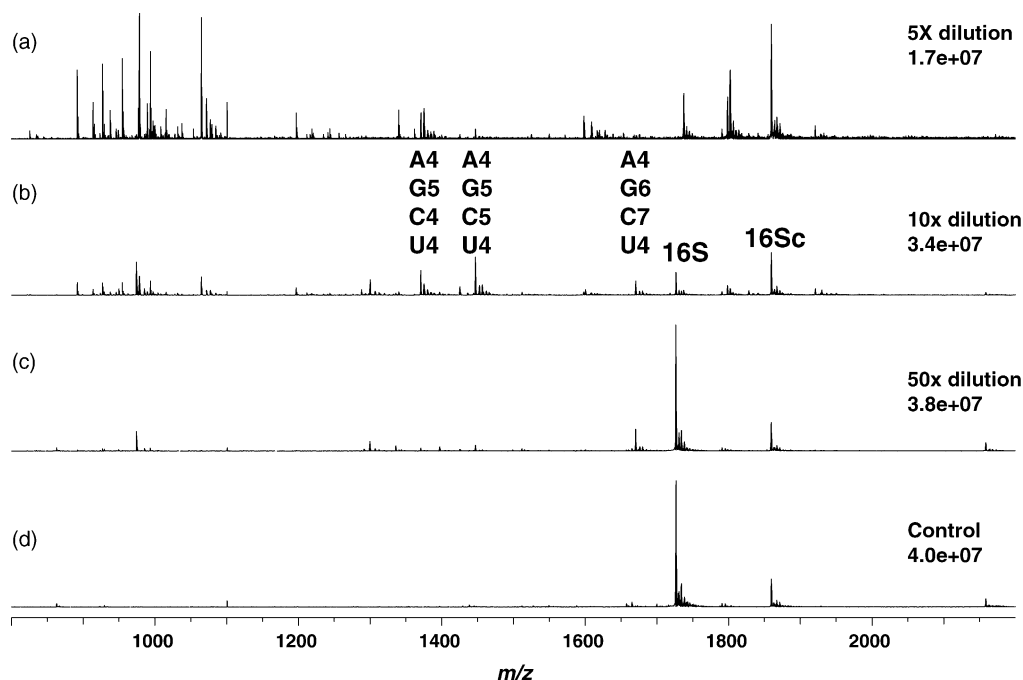


Fig. 7. ESI-FTICR mass spectra of a plant extract that exhibits selective degradation of the 27-mer 16S A-site RNA construct (**16S**). The extract was screened at (A) 5 $\times$ , (B) 10 $\times$ , and (C) 50 $\times$  dilutions from the original stock concentration. (D) A well in which no extract has been added. The abundances of the 28-mer control RNA construct (**16Sc**) are indicated at the right side of the figure. Until the 5 $\times$  dilution, the abundance of **16Sc** in wells containing the extract is similar to the well without extract.

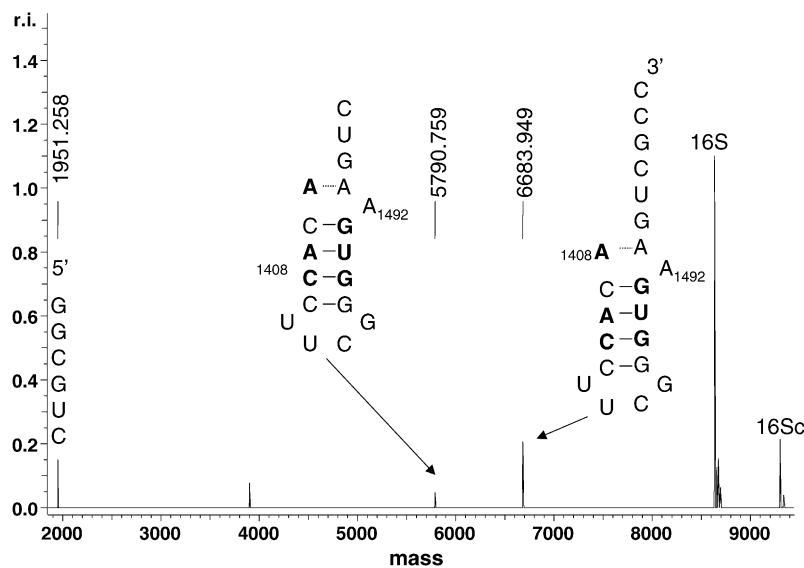


Fig. 8. Deconvoluted spectrum of the 50 $\times$  dilution of the extract. Based on base composition calculations, the corresponding sequence for the three cleavage products are shown.

studies are currently underway to identify the agent responsible for the cleavage activity.

#### 4. Conclusions

The MASS assay, which employs ESI-FTICR mass spectrometry to interrogate noncovalent ligand-target com-

plexes, represents an exciting platform for drug discovery. It has been shown that MASS can be used to examine synthetic compound libraries as well as natural product extracts for potential drug leads in a quick and robust manner. Although the MASS has been used to study ligand binding to structured RNA drug targets, this technique could easily be extended to protein drug targets.

## References

- [1] T. Herman, E. Westhof, *Combinatorial Chem. High-Throughput Screening* 3 (2000) 219.
- [2] S.J. Sucheck, C.-H. Wong, *Curr. Opin. Chem. Biol.* 4 (2000) 678.
- [3] A. Ramos, C.C. Gubser, G. Varani, *Curr. Opin. Struct. Biol.* 7 (1997) 317.
- [4] G.L. Conn, D.E. Draper, *Curr. Opin. Struct. Biol.* 8 (1998) 278.
- [5] R.T. Batey, R.P. Rambo, J.A. Doudna, *Angew. Chem. (Engl.)* 38 (1999) 2326.
- [6] D. Fourmy, M.I. Recht, S.C. Blanchard, J.D. Puglisi, *Science (Washington, D.C.)* 274 (1996) 1367.
- [7] M.I. Recht, D. Fourmy, S.C. Blanchard, K.D. Dahlquist, J.D. Puglisi, *J. Mol. Biol.* 262 (1996) 421.
- [8] Y. Wang, K. Hamasaki, R.R. Rando, *Biochemistry* 36 (1997) 768.
- [9] D. Fourmy, M.I. Recht, J.D. Puglisi, *J. Mol. Biol.* 277 (1998) 347.
- [10] D. Fourmy, S. Yoshizawa, J.D. Puglisi, *J. Mol. Biol.* 277 (1998) 333.
- [11] C.-H. Wong, M. Hendrix, E.S. Priestley, W.A. Greenberg, *Chem. Biol.* 5 (1998) 397.
- [12] M.I. Recht, S. Douthwaite, K.D. Dahlquist, J.D. Puglisi, *J. Mol. Biol.* 286 (1999) 33.
- [13] A.P. Carter, W.M. Clemons, D.E. Brodersen, R.J. Morgan-Warren, B.T. Wimberly, V. Ramakrishnan, *Nature* 407 (2000) 340.
- [14] B.T. Wimberly, D.E. Brodersen, W.M. Clemons, R.J. Morgan-Warren, A.P. Carter, C. Vonrhein, T. Hartsch, V. Ramakrishnan, *Nature* 407 (2000) 327.
- [15] D. Hyun Ryu, R.R. Rando, *Bioorg. Med. Chem.* 9 (2001) 601.
- [16] S.R. Lynch, J.D. Puglisi, *J. Mol. Biol.* 306 (2001) 1037.
- [17] Q. Vicens, E. Westhof, *J. Mol. Biol.* 326, 1175.
- [18] P. Purohit, S. Stern, *Nature* 370 (1994) 659.
- [19] R.H. Griffey, S.A. Hofstadler, K.A. Sannes-Lowery, D.J. Ecker, S.T. Croke, *Proc. Natl. Acad. Sci. U.S.A.* 96 (1999) 10129.
- [20] S.A. Hofstadler, K.A. Sannes-Lowery, S.T. Croke, D.J. Ecker, H. Sasmor, S. Manalili, R.H. Griffey, *Anal. Chem.* 71 (1999) 3436.
- [21] K.A. Sannes-Lowery, J.J. Drader, R.H. Griffey, S.A. Hofstadler, *TrAC, Trends Anal. Chem.* 19 (2000) 481.
- [22] K.A. Sannes-Lowery, R.H. Griffey, S.A. Hofstadler, *Anal. Biochem.* 280 (2000) 264.
- [23] S.A. Hofstadler, R.H. Griffey, *Curr. Opin. Drug Discov. Dev.* 3 (2000) 423.
- [24] R.H. Griffey, K.A. Sannes-Lowery, J.J. Drader, V. Mohan, E.E. Swayze, S.A. Hofstadler, *J. Am. Chem. Soc.* 122 (2000) 9933.
- [25] X. Cheng, R. Chen, J.E. Bruce, B.L. Schwartz, G.A. Anderson, S.A. Hofstadler, D.C. Gale, R.D. Smith, J. Gao, G.B. Sigal, *J. Am. Chem. Soc.* 117 (1995) 8859.
- [26] M.J. Greig, H. Gaus, L.L. Cummins, H. Sasmor, R.H. Griffey, *J. Am. Chem. Soc.* 117 (1995) 10765.
- [27] H.K. Lim, Y.L. Hsieh, B. Ganem, J. Henion, *J. Mass Spectrom.* 30 (1995) 708.
- [28] J. Gao, X. Cheng, R. Chen, G.B. Sigal, B.L. Schwartz, S.A. Hofstadler, G.A. Anderson, R.D. Smith, G.M. Whitesides, *J. Med. Chem.* 39 (1996) 1949.
- [29] Q.Y. Gao, X.H. Cheng, R.D. Smith, C.F. Yang, I.H. Goldberg, *J. Mass Spectrom.* 31 (1996) 31.
- [30] Q. Wu, X. Cheng, S.A. Hofstadler, R.D. Smith, *J. Mass Spectrom.* 31 (1996) 669.
- [31] Q.Y. Wu, J.M. Gao, D. Josephmccarthy, G.B. Sigal, J.E. Bruce, G.M. Whitesides, R.D. Smith, *J. Am. Chem. Soc.* 119 (1997) 1157.
- [32] J.A. Loo, P. Hu, P. McConnell, W.T. Mueller, *J. Am. Soc. Mass Spectrom.* 8 (1997) 234.
- [33] R.D. Smith, J.E. Bruce, Q. Wu, Q.P. Lei, *Chem. Soc. Rev.* 26 (1997) 191.
- [34] A. Ayed, A. Krutchinsky, I.V. Chernushevich, W. Ens, H.W. Duckworth, K.G. Standing, *NATO ASI Ser., Ser. C* 510 (1998) 135.
- [35] A. Ayed, A.N. Krutchinsky, W. Ens, K.G. Standing, H.W. Duckworth, *Rapid Commun. Mass Spectrom.* 12 (1998) 339.
- [36] T.J.D. Jorgensen, P. Roepstorff, *Anal. Chem.* 70 (1998) 4427.
- [37] J.A. Loo, K.A. Sannes-Lowery, P. Hu, D.P. Mack, H.-Y. Mei, in: W. Ens, K.G. Standing, I.V. Chernushevich (Eds.), *New Methods for the Study of Biomolecular Complexes*, vol. 510, Dordrecht, Kluwer, 1998, p. 83.
- [38] J.A. Loo, K.A. Sannes-Lowery, *Mass Spectrom. Biol. Mater. (second ed.)* (1998) 345.
- [39] S.A. Hofstadler, R.H. Griffey, *Chem. Rev.* 101 (2001) 377.
- [40] D.J. Winzor, W.H. Sawyer, *Quantitative Characterization of Ligand Binding*, 1995.
- [41] L.L. Cummins, S. Chen, L.B. Blyn, K.A. Sannes-Lowery, J.J. Drader, R.H. Griffey, S.A. Hofstadler, *J. Nat. Prod.* 66 (9) (2003) 1186.
- [42] D.C. DeJongh, J.D. Hribar, S. Hanessian, P.W.K. Woo, *J. Am. Chem. Soc.* 89 (1967) 3364.
- [43] O. Curcuruto, G. Kennedy, M. Hamdan, *Org. Mass Spectrom.* 29 (1994) 547.
- [44] B.J. Goolsby, J.S. Brodbelt, *J. Mass Spectrom.* 35 (2000) 1011.
- [45] J.J. Drader, G.A. Anderson, Y. Jiang, J.C. Hannis, S.A. Hofstadler, manuscript in preparation, 2002.